

See discussions, stats, and author profiles for this publication at: <https://www.researchgate.net/publication/264248437>

Optical Nonlinearity in $\text{Cu}_2\text{CdSnS}_4$ and $\alpha/\beta\text{-Cu}_2\text{ZnSiS}_4$: Diamond-like Semiconductors with High Laser-Damage Thresholds

ARTICLE in INORGANIC CHEMISTRY · JULY 2014

Impact Factor: 4.76 · DOI: 10.1021/ic501310d · Source: PubMed

CITATIONS

7

READS

60

10 AUTHORS, INCLUDING:



Jacilynn A. Brant

Duquesne University

16 PUBLICATIONS 51 CITATIONS

SEE PROFILE



Yong Soo Kim

University of Ulsan

60 PUBLICATIONS 198 CITATIONS

SEE PROFILE



Joon I. Jang

Binghamton University

70 PUBLICATIONS 1,057 CITATIONS

SEE PROFILE



Jennifer A Aitken

Duquesne University

95 PUBLICATIONS 693 CITATIONS

SEE PROFILE

Optical Nonlinearity in $\text{Cu}_2\text{CdSnS}_4$ and $\alpha/\beta\text{-Cu}_2\text{ZnSiS}_4$: Diamond-like Semiconductors with High Laser-Damage ThresholdsKimberly A. Rosmus,[†] Jacilynn A. Brant,[†] Stephen D. Wisneski,[†] Daniel J. Clark,[‡] Yong Soo Kim,^{‡,§} Joon I. Jang,[‡] Carl D. Brunetta,[†] Jian-Han Zhang,[†] Matthew N. Srncic,[†] and Jennifer A. Aitken^{*,†}[†]Department of Chemistry and Biochemistry, Duquesne University, Pittsburgh, Pennsylvania 15282, United States[‡]Department of Physics, Applied Physics and Astronomy, Binghamton University, P.O. Box 6000, Binghamton, New York 13902, United States[§]Department of Physics and Energy Harvest-Storage Research Center, University of Ulsan, Ulsan 680-749, South Korea

S Supporting Information

ABSTRACT: $\text{Cu}_2\text{CdSnS}_4$ and $\alpha/\beta\text{-Cu}_2\text{ZnSiS}_4$ meet several criteria for promising nonlinear optical materials for use in the infrared (IR) region. Both are air-stable, crystallize in noncentrosymmetric space groups, and possess high thermal stabilities. $\text{Cu}_2\text{CdSnS}_4$ and $\alpha/\beta\text{-Cu}_2\text{ZnSiS}_4$ display wide ranges of optical transparency, 1.4–25 and 0.7–25 μm , respectively, and have relatively large second-order nonlinearity as well as phase matchability for wide regions in the IR. The laser-damage threshold (LDT) for $\text{Cu}_2\text{CdSnS}_4$ is 0.2 GW/cm^2 , whereas $\alpha/\beta\text{-Cu}_2\text{ZnSiS}_4$ has a LDT of 2.0 GW/cm^2 for picosecond near-IR excitation. Both compounds also exhibit efficient third-order nonlinearity. Electronic structure calculations provide insight into the variation in properties.

Improved nonlinear optical (NLO) materials for infrared (IR) applications are essential to advancing telecommunications, biomedical imaging, and diagnostics, such as the detection of trace gases.¹ Some of the criteria for ideal NLO materials are high optical nonlinearity, extreme optical transparency, environmental stability, large laser-damage threshold (LDT), and high thermal stability.² Thus, the quest for “ideal” NLO materials proves challenging. Although there are several attractive NLO crystals for use in the ultraviolet (UV), visible (vis), and near-IR (NIR) regions,³ there are fewer options for use further in the IR,² and no one material offers radiation in the entire region.

Although several commercial NLO crystals are useful for mid-IR generation, each suffers drawbacks. For operation of a 2 μm pumped optical parametric oscillator at wavelengths between 2 and 8 μm , ZnGeP_2 is used because it is transparent and phase-matchable (PM) at 2 μm and has a large $\chi^{(2)}$ value of 150 pm/V yet is limited at longer wavelengths because of multiple photon absorption.^{2b} Therefore, in the region of $\sim 9\text{--}11\text{ }\mu\text{m}$, AgGaSe_2 is used for wavelength (λ) conversion; however, it is plagued by two-photon absorption (2PA) and has inadequate birefringence for 1 μm phase matching.^{2b} AgGaS_2 is PM at 1 μm with a $\chi^{(2)}$ value of 36 pm/V ; however, it has a low LDT because of 2PA.^{2b}

Some new materials show potential in IR NLO applications.⁴ For example, $\text{Ba}_8\text{Sn}_4\text{S}_{15}$ has wide optical transparency, a $\chi^{(2)}$ value of 23.92 pm/V , and a LDT that is ~ 26 times that of AgGaS_2 when irradiated with a 1.064 μm laser; however, it is non-phase-

matchable (NPM) at 2.05 μm .^{4b} NaAsSe_2 shows strong second-harmonic generation (SHG) but is NPM at 1.58 μm .^{4c} The $\text{ACd}_4\text{In}_5\text{Se}_{12}$ ($A = \text{Rb}, \text{Cs}$) compounds exhibit wide optical transparency and SHG responses $\sim 35\text{--}40$ times those of AgGaS_2 at 2.05 μm , but are also NPM at 2.05 μm .^{4d} Practical applications require improved materials accessible by robust design.

Because the discovery of compounds for SHG applications is contingent on noncentrosymmetric (NCS) structures, many strategies utilize exploratory synthesis involving acentric building units.^{4,5} This approach, although appealing for unexpected and interesting structures, is a gamble for finding NCS materials because acentric building units often pack into centrosymmetric structures. In contrast, diamond-like semiconductors (DLSs) provide a reliable route to attractive SHG materials because their compositions are predictable and the structures are inherently NCS because the MS_4 tetrahedra align in one direction.⁶ Additionally, DLSs provide chemical flexibility that can be exploited to tune properties, such as phase matching and refractive index.^{7,8} High optical nonlinearity arises in DLSs as a consequence of predominantly covalent bonding. Indeed, DLSs dominate the list of commercially available materials, e.g., AgGaS_2 , AgGaSe_2 , and ZnGeP_2 .²

In 1981, Pamplin predicted compositions of multinary DLSs and stated that “there are a thousand adamantite [diamond-like] phases from which to choose device material. [The] crystal growth and characterization should continue in as many laboratories as possible.”⁹ Here, using $\text{Cu}_2\text{CdSnS}_4$ and $\alpha/\beta\text{-Cu}_2\text{ZnSiS}_4$,¹⁰ we demonstrate how a change from Sn to Si for the IV ion in the $\text{I}_2\text{--II--IV--VI}_4$ formula can have significant effects on key characteristics critical for NLO applications. Establishing structure–property correlations is imperative for directing efforts toward the most promising materials.

The structure of $\text{Cu}_2\text{CdSnS}_4$ was determined using single-crystal X-ray diffraction. The compound crystallizes with the stannite structure, a derivative of cubic diamond. This is in close agreement with the structure of the mineral cernyite, $\text{Cu}_2\text{Cd}_{0.37}\text{Zn}_{0.33}\text{Fe}_{0.29}\text{Mn}_{0.005}\text{SnS}_4$,¹¹ and the reported lattice parameters.¹² The wurtz-stannite structure of $\alpha\text{-Cu}_2\text{ZnSiS}_4$ and the wurtz-kesterite structure of $\beta\text{-Cu}_2\text{ZnSiS}_4$ are derived from

Received: June 4, 2014

Published: July 25, 2014



hexagonal diamond.¹⁰ Although every S^{2-} is surrounded by one Zn^{2+} or Cd^{2+} , one Si^{4+} or Sn^{4+} , and two Cu^+ ions in each compound, the cation ordering patterns differ (Figure 1).

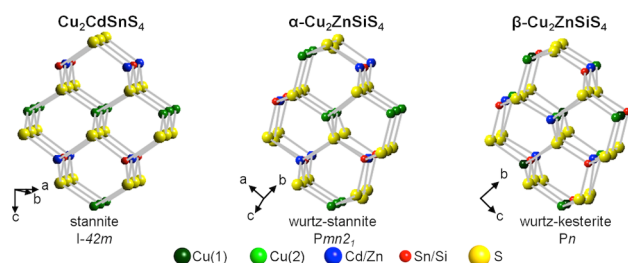


Figure 1. Three-dimensional diamond-like structures.

Synchrotron powder diffraction indicates that Cu_2CdSnS_4 is nearly phase pure and that the $\sim 60:40$ α - and β - Cu_2ZnSiS_4 sample contains $\sim 0.3\%$ ZnS (Figure S1, Supporting Information). Thus far, α - and β - Cu_2ZnSiS_4 have not been isolated because of similar ground-state energies that impose synthetic limitations.^{10b} Cu_2CdSnS_4 melts congruently at $930^\circ C$, and α/β - Cu_2ZnSiS_4 exhibits higher thermal stability with a melting point over $1000^\circ C$ (Figure S3, Supporting Information). Cu_2CdSnS_4 was found to have an optical band gap of 0.92 eV (Figure S4, Supporting Information). The band gaps have been estimated to be ~ 3.0 and ~ 3.2 eV for α - and β - Cu_2ZnSiS_4 , respectively.^{10b}

The title compounds exhibit wide optical transparency, exceeding $AgGaSe_2$ (0.76 – $17\ \mu m$), $AgGaS_2$ (0.48 – $11.4\ \mu m$), and $ZnGeP_2$ (0.74 – $12\ \mu m$).^{2b} Cu_2CdSnS_4 and α/β - Cu_2ZnSiS_4 are transparent from 1.4 to $25\ \mu m$ and from 0.7 to $25\ \mu m$, respectively (Figure 2). Although some new SHG materials have narrower transparency windows, such as $Na_2Ge_2Se_5$ ^{4f} and $K_2P_2Se_6$,^{4g} others have comparable ranges.^{4b,d}

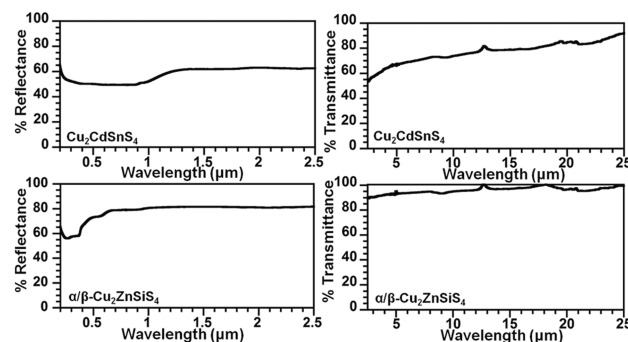


Figure 2. UV-vis-NIR (left) and Fourier transform IR (right) spectra.

The phase matchability of Cu_2CdSnS_4 and α/β - Cu_2ZnSiS_4 was evaluated by measuring SHG with a broadband incident λ of 1100 – 3300 nm ($\lambda_{SHG} = 550$ – 1650 nm) for particle sizes ≤ 106 and $\leq 150\ \mu m$, respectively (Figure S5, Supporting Information). The SHG response for Cu_2CdSnS_4 rises with increasing particle size (i.e., is PM) at $\lambda_{SHG} \geq 1050$ nm (Figure S6, Supporting Information).¹³ α/β - Cu_2ZnSiS_4 has a larger range of phase matchability, $\lambda_{SHG} \geq 850$ nm (Figure S7, Supporting Information). These PM regions, which are wider than $AgGaSe_2$ ($\lambda_{SHG} \geq 1550$ nm), can benefit wave-mixing applications.¹⁴ Using $AgGaSe_2$ as a reference, the $\chi^{(2)}$ values of Cu_2CdSnS_4 and α/β - Cu_2ZnSiS_4 were found to be 62 ± 3 and 15 ± 2 pm/V, respectively (Figure 3). The $\chi^{(2)}$ value of Cu_2CdSnS_4 is

comparable to that of $AgGaSe_2$ (66 pm/V) and notably larger than that of $AgGaS_2$.

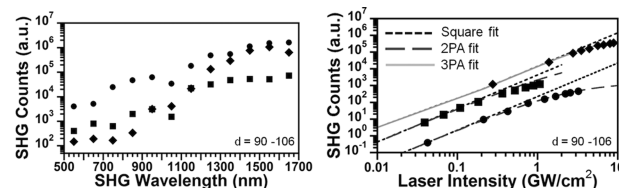


Figure 3. Broadband SHG and SHG power dependence of Cu_2CdSnS_4 (■), α/β - Cu_2ZnSiS_4 (◆), and $AgGaSe_2$ (●). For power dependence, $\lambda = 1064$ nm for ● and ◆; $\lambda = 1300$ nm for ■.

Third-order nonlinearity is attractive for applications in all-optical switching and optical image processing in the visible and IR regions.¹⁵ The potential of the title compounds for these types of applications was examined by measuring third-harmonic generation (THG), and the $\chi^{(3)}$ values were estimated by the powder method.^{5f} Whereas SHG materials are commonly used in frequency-mixing setups to access wider frequency ranges, THG materials can greatly improve processing speeds.

The THG responses (Figure S8, Supporting Information) for the samples and $AgGaSe_2$ all intensify with increasing λ . The THG efficiencies likely improve in the deeper mid-IR, especially for Cu_2CdSnS_4 because all of the THG responses were measured above the band gap. Because of band-gap absorption, the $\chi^{(3)}$ value for Cu_2CdSnS_4 [$(8.0 \pm 2.0) \times 10^4$ pm²/V²] is likely underestimated. Owing to the wide band gap of α/β - Cu_2ZnSiS_4 , the THG efficiency [$\chi^{(3)} = (2.1 \pm 0.6) \times 10^4$ pm²/V²] is unrestricted in the measured region. It was confirmed that THG is NPM for both compounds as well as the reference for $\lambda = 1300$ – 3100 nm (Figure S9, Supporting Information), which is typical because of a large phase mismatch between λ and λ_{THG} . Although these $\chi^{(3)}$ values are lower than that of $AgGaSe_2$ (1.6×10^5 pm²/V²), practical use in applications relies on high LDT.

To assess LDTs, spectrally integrated SHG counts for Cu_2CdSnS_4 and α/β - Cu_2ZnSiS_4 were plotted versus input intensity under picosecond laser excitation (Figure 3). Each dashed line represents the maximum SHG case where fundamental depletion is absent. Although Cu_2CdSnS_4 has high $\chi^{(2)}$ and $\chi^{(3)}$ values, it suffers serious damage upon picosecond laser exposure because of one-photon absorption at 1064 nm (Figure S10, Supporting Information). The LDT of Cu_2CdSnS_4 (0.2 GW/cm² at 1300 nm) is akin to that of $AgGaSe_2$ (0.2 GW/cm² at 1064 nm). The LDT of α/β - Cu_2ZnSiS_4 (2.0 GW/cm²) is 1 order of magnitude larger than that of $AgGaSe_2$. This progress is credited to the wide band gap because laser damage results from three-photon absorption (3PA).

An electronic structure calculation was reported for Cu_2CdSnS_4 ,¹⁶ but here we expand upon the partial density of states (PDOS) in addition to using the modified Becke–Johnson exchange potential for all compounds (Table S4, Supporting Information).¹⁷ The direct band gaps of Cu_2CdSnS_4 , α - Cu_2ZnSiS_4 and β - Cu_2ZnSiS_4 were calculated as 0.79 , 2.05 , and 2.57 eV, respectively. The differences in the electronic structures of Cu_2CdSnS_4 and α/β - Cu_2ZnSiS_4 can be understood by examining the PDOS (Figures 4 and S11 and S12, Supporting Information). The largest discrepancy near the Fermi level (E_F) arises from the contributions of the IV ion orbitals at the conduction band minimum (CBM). For α - Cu_2ZnSiS_4 , the states at the CBM chiefly arise from the S p , Si s , Si p , and Zn s orbitals, with lesser contributions from the Zn p and Cu p orbitals; the

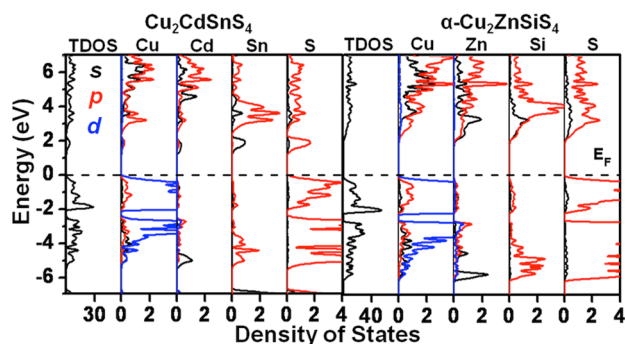


Figure 4. Total density of states (TDOS) and PDOS (electrons/eV). The dotted line denotes the Fermi level (E_F).

PDOS for β - $\text{Cu}_2\text{ZnSiS}_4$ is similar to that of α - $\text{Cu}_2\text{ZnSiS}_4$ (Figures S11 and S12, Supporting Information). However, in $\text{Cu}_2\text{CdSnS}_4$, the lowest energy states in the CBM evolve predominantly from the Sn s and S p orbitals. For the title compounds, the largest disparity of Mulliken bond populations arises in the IV–S bonds, where the Sn–S bond order is 0.49 and that of Si–S is ~ 0.7 (Table S3, Supporting Information).

In summary, $\text{Cu}_2\text{CdSnS}_4$ and α/β - $\text{Cu}_2\text{ZnSiS}_4$ meet critical criteria for useful NLO materials. The $\chi^{(2)}$, $\chi^{(3)}$, and LDT values of $\text{Cu}_2\text{CdSnS}_4$ are similar to those of AgGaSe_2 . Although the $\chi^{(2)}$ and $\chi^{(3)}$ values of α/β - $\text{Cu}_2\text{ZnSiS}_4$ are lower, it outshines benchmark IR NLO materials in LDT. These results align with the ideas that a narrower band gap leads to larger optical nonlinearity,¹⁸ whereas a wider band gap yields better LDT. Yet, high NLO susceptibility and LDT are not mutually exclusive. Indeed, we recently revealed strong SHG, THG, and LDT for $\text{Li}_2\text{CdGeS}_4$.¹⁹ To access useful NLO materials, a firmer grasp on the interplay between bonding, band gap, NLO susceptibility, and LDT must be established. In this system, we propose that improvements could be accomplished by tuning the composition to increase the level of covalency without much change in the band gap (i.e., states near E_F).

■ ASSOCIATED CONTENT

■ Supporting Information

Experimental details, X-ray diffraction, Rietveld refinement, SHG, THG, LDT, thermal analysis, and electronic structure. This material is available free of charge via the Internet at <http://pubs.acs.org>.

■ AUTHOR INFORMATION

Corresponding Author

*E-mail: aikenj@duq.edu.

Notes

The authors declare no competing financial interest.

■ ACKNOWLEDGMENTS

This work was supported by the National Science Foundation (grant DMR-1201729). Use of the Advanced Photon Source, an Office of Science User Facility operated by the U.S. Department of Energy (DOE), Office of Science, by Argonne National Laboratory, was supported by the U.S. DOE under contract DE-AC02-05CH11357. Y.S.K. acknowledges support from the Basic Science Research Program (2014-010369) and Priority Research Center Program (2009-0093818) through the NRF of Korea funded by the Ministry of Education.

■ REFERENCES

- (1) (a) Cotter, D.; Manning, R. J.; Blow, K. J.; Ellis, A. D.; Kelly, A. E.; Nasset, D.; Phillips, I. D.; Poustie, A. J.; Rogers, D. C. *Science* **1999**, *286*, 1523–1528. (b) Zipfel, W. R.; Williams, R. M.; Webb, W. W. *Nat. Biotechnol.* **2003**, *21*, 1369–1377. (c) Pushkarsky, M.; Tsekoun, A.; Dunayevskiy, I. G.; Go, R.; Patel, C. K. N. *Proc. Natl. Acad. Sci. U.S.A.* **2006**, *103*, 10846–10849.
- (2) (a) Ohmer, M. C.; Pandey, R. *MRS Bull.* **1998**, *23*, 16–22. (b) Schunemann, P. G. *Proc. SPIE* **2007**, *6455*, 64550R.
- (3) (a) Wu, H.; Yu, H.; Pan, S.; Huang, Z.; Yang, Z.; Su, X.; Poeppelmeier, K. R. *Angew. Chem., Int. Ed.* **2013**, *52*, 3406–3410. (b) Sasaki, S.; Mori, Y.; Yoshimura, M.; Yap, Y. K.; Kamimura, T. *Mater. Sci. Eng., R* **2000**, *30*, 1–54. (c) Wang, K.; Fang, C.; Zhang, J.; Sun, X.; Wang, S.; Gu, Q.; Zhao, X.; Wang, B. *J. Cryst. Growth* **2006**, *287*, 478–482.
- (4) (a) Chung, I.; Kanatzidis, M. G. *Chem. Mater.* **2014**, *26*, 849–869. (b) Luo, Z.-Z.; Lin, C.-S.; Zhang, W.-L.; Zhang, H.; He, Z.-Z.; Cheng, W.-D. *Chem. Mater.* **2014**, *26*, 1093–1099. (c) Bera, T. K.; Jang, J. I.; Song, J.-H.; Malliakas, C. D.; Freeman, A. J.; Ketterson, J. B.; Kanatzidis, M. G. *J. Am. Chem. Soc.* **2010**, *132*, 3484–3495. (d) Lin, J.; Chen, L.; Zhou, L.-J.; Wu, L.-M. *J. Am. Chem. Soc.* **2013**, *135*, 12914–12921. (e) Zhu, T.; Chen, X.; Qin, J. *Front. Chem. China* **2011**, *6*, 1–8. (f) Badikov, V. V.; Laptev, V. B.; Panyutin, V. L.; Ryabov, E. A.; Shevyrdayeva, G. S. *Quantum Electron.* **2005**, *35*, 263–267. (g) Chung, I.; Malliakas, C. D.; Jang, J. I.; Canlas, C. G.; Weliky, D. P.; Kanatzidis, M. G. *J. Am. Chem. Soc.* **2007**, *129*, 14996–15006.
- (5) (a) Zou, G.; Huang, L.; Ye, N.; Lin, C.; Cheng, W.; Huang, H. *J. Am. Chem. Soc.* **2013**, *135*, 18560–18566. (b) Li, P. X.; Hu, C. L.; Zu, X.; Wang, R. Y.; Sun, C. F.; Mao, J. G. *Inorg. Chem.* **2010**, *49*, 4599–4605. (c) Yin, W.; Feng, K.; Hao, W.; Yao, J.; Wu, Y. *Inorg. Chem.* **2012**, *51*, 5839–5843. (d) Lu, H.; Gautier, R.; Donakowski, M. D.; Tran, T. T.; Edwards, B. W.; Nino, J. C.; Halasyamani, P. S.; Liu, Z.; Poeppelmeier, K. R. *J. Am. Chem. Soc.* **2013**, *135*, 11942–11950. (e) Kim, S. H.; Yeon, J.; Halasyamani, P. S. *Chem. Mater.* **2009**, *21*, 5335–5342. (f) Jang, J. I.; Haynes, A. S.; Saouma, F. O.; Otieno, C. O.; Kanatzidis, M. G. *Opt. Mater. Express* **2013**, *3*, 1302–1312.
- (6) (a) Parthé, E. *Crystal Chemistry of Tetrahedral Structures*; Gordon and Breach Science Publishers, Inc.: New York, 1964. (b) Goryunova, N. A. *The Chemistry of Diamond-Like Semiconductors*; Massachusetts Institute of Technology: Cambridge, MA, 1965.
- (7) (a) Bhar, G. C.; Das, S.; Chatterjee, U.; Datta, P. K.; Andreev, Y. N. *Appl. Phys. Lett.* **1993**, *63*, 1316–1318. (b) Badikov, V. V.; Laptev, V. B.; Panyutin, V. L.; Ryabov, E. A.; Shevyrdayeva, G. S. *Quantum Electron.* **2005**, *35*, 263–267.
- (8) Huang, J.-J.; Atuchin, V. V.; Andreev, Y. M.; Lanski, G. V.; Pervukhina, N. V. *J. Cryst. Growth* **2006**, *292*, 500–504.
- (9) Pamplin, B. *Prog. Cryst. Growth Charact.* **1981**, *3*, 179–192.
- (10) (a) Rosmus, K. A.; Aitken, J. A. *Acta Crystallogr., Sect. E* **2011**, *67*, i28. (b) Rosmus, K. A.; Brunetta, C. D.; Srnc, M. N.; Karuppannan, B.; Aitken, J. A. *Z. Anorg. Allg. Chem.* **2012**, *638*, 2578–2584.
- (11) Szymanski, J. T. *Can. Mineral.* **1978**, *16*, 146–151.
- (12) (a) Nitsche, R.; Sargent, D. F.; Wild, P. J. *Cryst. Growth* **1967**, *1*, 52–53. (b) Schäfer, W.; Nitsche, R. *Mater. Res. Bull.* **1974**, *9*, 645–654.
- (13) Ok, K. M.; Chi, E. O.; Halasyamani, P. S. *Chem. Soc. Rev.* **2006**, *35*, 710–717.
- (14) (a) Witte, T.; Kompa, K. L.; Motzkus, M. *Appl. Phys. B: Lasers Opt.* **2003**, *76*, 467–471. (b) Chatterjee, U.; Kumbhakar, P.; Chaudhary, A. K.; Bhar, G. C. *Appl. Phys. B: Lasers Opt.* **2001**, *72*, 407–409.
- (15) Fuentes-Herandez, C.; Ramos-Ortiz, G.; Tseng, S.-Y.; Gaj, M. P.; Kippelen, B. *J. Mater. Chem.* **2009**, *19*, 7394–7401.
- (16) Xiao, Z.-Y.; Li, Y.-F.; Yao, B.; Deng, R.; Ding, Z.-H.; Wu, T.; Yang, G.; Li, C.-R.; Dong, Z.-H.; Liu, L.; Zhang, L.-G.; Zhao, H.-F. *J. Appl. Phys.* **2013**, *114*, 183506.
- (17) Koller, D.; Tran, F.; Blaha, P. *Phys. Rev. B* **2011**, *83*, 195134.
- (18) Levine, B. F. *Phys. Rev. B* **1973**, *7*, 2600–2626.
- (19) (a) Brant, J. A.; Clark, D. J.; Kim, Y. S.; Jang, J. I.; Zhang, J.-H.; Aitken, J. A. *Chem. Mater.* **2014**, *26*, 3045–3048. (b) Jang, J. I.; Clark, D. J.; Brant, J. A.; Aitken, J. A.; Kim, Y. S. *Opt. Lett.*, in press.